

Supporting Information

Solar-powered plasmon-boosted graphene towards enhanced ammonia production

Manpreet Kaur^a, Avinash Alagumalai^a, Rad Sadri^a, Saana Tandon^{a,b}, Sameh M. Osman^c, Edward P.L. Roberts^a, Hua Song^{a*}

^aDepartment of Chemical and Petroleum Engineering, University of Calgary, 2500 University Drive, NW, Calgary, Alberta, T2N 1N4, Canada

^bDepartment of Chemistry, Indian Institute of Technology Roorkee, Roorkee, Uttarakhand 247667, India

^cChemistry Department, College of Science, King Saud University, P.O. Box 2455, Riyadh 11451, Saudi Arabia

*Corresponding author: E-mail: sonh@ucalgary.ca ([Hua Song](mailto:sonh@ucalgary.ca))

Table of contents: (Total pages. 7; figures. 10, Table 1)

1. Photograph capturing the experimental arrangement.
2. (a) Reaction product collection using Nessler reagent from PtRu@TiN/NG, (b) calibration curve used for estimation of NH₃ concentration. The absorbance at 420 nm was measured by UV-vis spectrophotometer.
3. TEM image of (a) pure monolayer N doped graphene i.e., NG (b) Corresponding SAED pattern (c) TiN NPs.
4. EPR spectra of PtRu@TiN/NG sample at room temperature.
5. Micro-GC of NRR gas products collected after the 60 min reaction.
6. Hydrazine detection using a para-(dimethylamino) benzaldehyde color reagent, with absorbance measured at 455 nm. PtRu@TiN/NG exhibited no detectable hydrazine signal.
7. (a) ¹⁵N₂ isotope labelling experiment for the NRR, (b) MALDI-MS spectra for the qualitative isotope labelling test.
8. Plot depicting the current-time profile of the PtRu@TiN/NG electrode, recorded at -1 V in an N₂ environment with light exposure for a duration of 10 hours.
9. Effective electrochemical active surface area tests (ECSA) of (a) PtRu@TiN, (b) PtRu@Graphene, and (c) PtRu@TiN/Graphene.

Table 1. Inductively coupled plasma mass spectrometry (ICP–MS) analysis of Pt and Ru loading on TiN/NG.

Table 2. A summary of the reported studies on the N₂ reduction to NH₃ by Photo-electro-catalysis.

Table S1. Inductively coupled plasma mass spectrometry (ICP–MS) analysis of Pt and Ru loading on TiN/NG

Sample	Pt	Ru
PtRu@TiN/NG	1.10 Wt.%	1.0 Wt.%
Pt@TiN/NG	2.05 Wt.%	xx
Ru@TiN/NG	xx	2.1 Wt.%

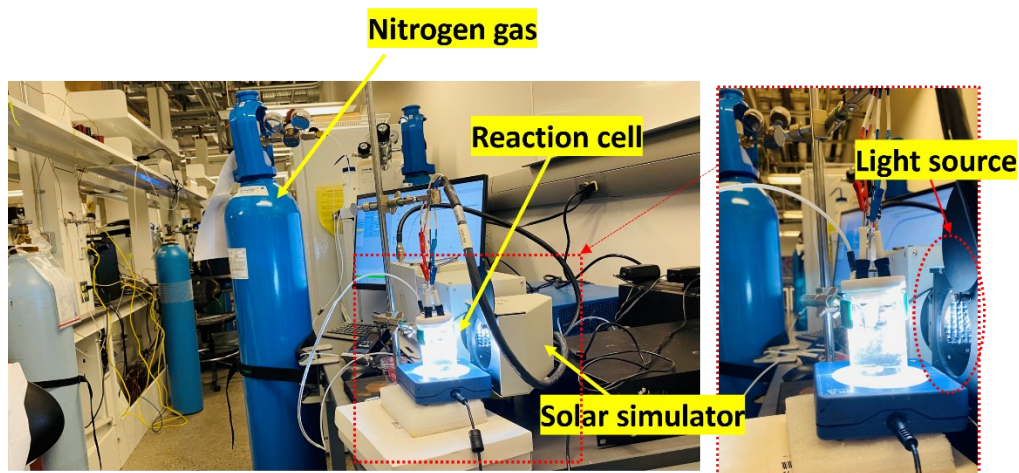


Figure S1. Photograph capturing the experimental arrangement.

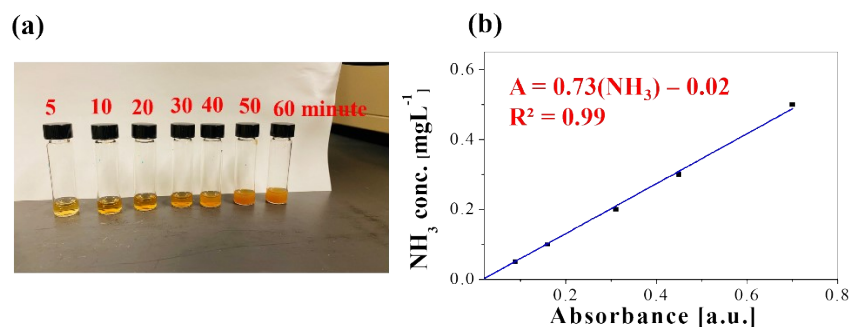


Figure S2. (a) Reaction product collection using Nessler reagent from PtRu@TiN/NG, (b) calibration curve used for estimation of NH_3 concentration. The absorbance at 420 nm was measured by UV-vis spectrophotometer.

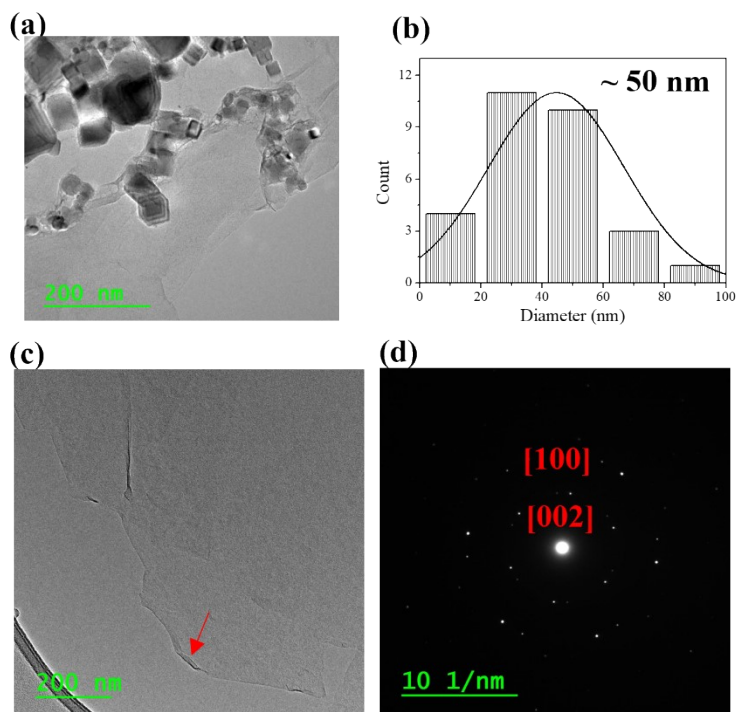


Figure S3. TEM image of (a-b) TiN NPs and its histogram illustrating the size distribution (c) pure monolayer N doped graphene i.e., NG indicated by arrow, (d) corresponding SAED pattern.

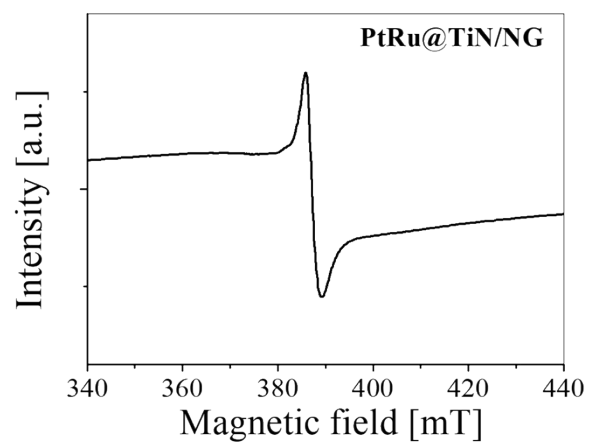


Figure S4. EPR spectra of PtRu@TiN/NG sample at room temperature.

Conditions	H ₂	O ₂	N ₂	NH ₃ ($\mu\text{mol h}^{-1}\cdot\text{mg}^{-1}_{\text{cat}}$)
-0.5V	ND	0.8%	99.2%	198
-1V	0.08	0.82%	99.1%	316
-1.5V	0.21%	0.78%	99.01%	301

Figure S5. Micro-GC of NRR gas products collected after the 60 min reaction.

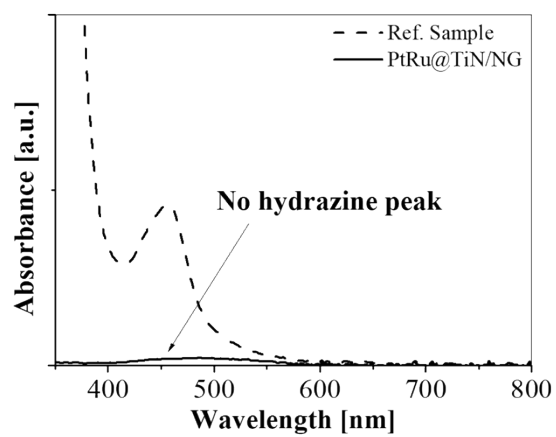


Figure S6. Hydrazine detection using a para-(dimethylamino) benzaldehyde color reagent, with absorbance measured at 455 nm. PtRu@TiN/NG exhibited no detectable hydrazine signal.

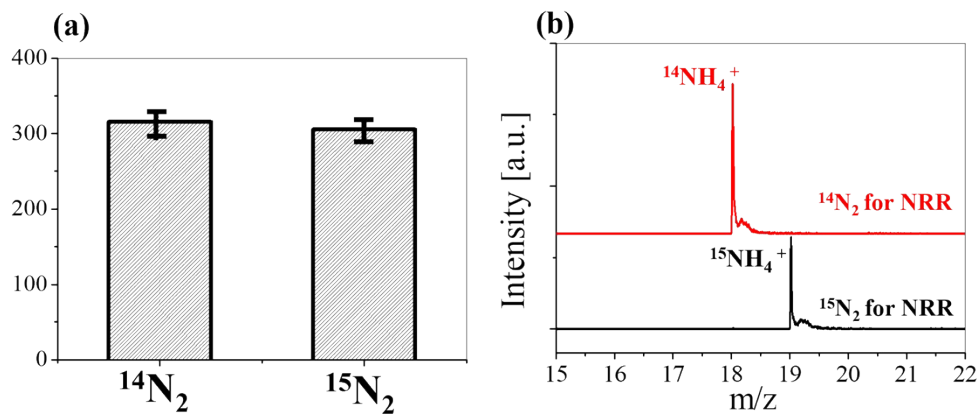


Figure S7. (a) $^{15}\text{N}_2$ isotope labelling experiment for the NRR, (b) MALDI-MS spectra for the qualitative isotope labelling test.

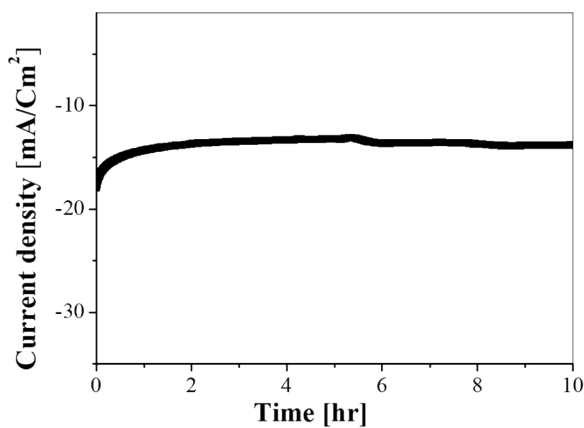


Figure S8. Plot depicting the current-time profile of the PtRu@TiN/NG electrode, recorded at -1 V in an N_2 environment with light exposure for a duration of 10 hours.

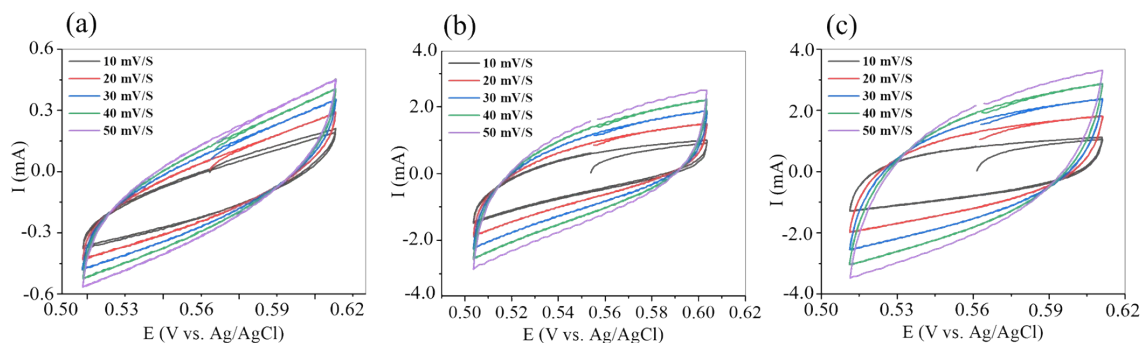


Figure S9. Effective electrochemical active surface area tests (ECSA) of (a) PtRu@TiN, (b) PtRu@NG, and (c) PtRu@NG.

Table S2. An overview of the documented research on the photo-electro-catalytic conversion of N_2 to NH_3 .

Catalysts	Light sources	Electrolytes	NH_3 yield rates	Ref.
PtRu@TiN/NG	2 suns illumination	N_2 - saturated H_2SO_4 in H_2O , Sacrificial reagent: Methanol	$316 \mu g \cdot h^{-1} \cdot mg_{cat}^{-1}$	This work
Pt-TiN/ C_3N_4	1 sun illumination	N_2 - saturated H_2SO_4 in H_2O , -1V Vs. Hg/ SO_4	$105 \mu g \cdot h^{-1} \cdot mg_{cata}^{-1}$	1
Black Silicon	2-sun illumination	N_2 -saturated Na_2SO_3 in H_2O , -1 V Vs. Ag/AgCl	$13.3 mg m^{-2} h^{-1}$	2
Cs 2O/Os-Au	UV-Visible	N_2/H_2	$2685 \mu mol g^{-1} h^{-1}$	3
TiO_2 - Cu_2O /Ru	150-W Xenon lamp	N_2 -saturated Na_2SO_4 in H_2O	$37.4 \mu g \cdot mg_{cat}^{-1} h^{-1}$	4
reduced graphene oxide	N/A	N_2 -saturated HCl in H_2O at -0.1V vs RHE	$7.3 \mu g \cdot mg_{cat}^{-1} h^{-1}$	5

NiO-Au-TiO ₂	532 nm CW laser, 43.8 mW/cm ²	0.2 M KNO ₃ electrolyte, -1.2 V vs Ag/AgCl,	80 μmol · L ⁻¹	6
Au embedded in hollow carbon nitride sphere	Xenon lamp at 420 nm cutoff filter	N ₂ -saturated in H ₂ O	783.4 μmol g ⁻¹ h ⁻¹	7
BaONCS-TNS		KNO ₃ Sacrificial reagent: ethylene glycol, -1.0 to 1.5 V vs. RHE	11.97 mol g _{metal} ⁻¹ h ⁻¹	8
Au nanoparticles		0.1M Li ₂ SO ₄ , -0.3 V vs. RHE	9.2 μg h ⁻¹ cm ⁻²	9

Reference

1. Kaur, M.; Faizan, M.; Song, H., Plasmonic titanium nitride based ammonia synthesis by Photoelectrocatalytic reduction of nitrogen. *Chemical Engineering Journal* **2023**, 145963.
2. Ali, M.; Zhou, F.; Chen, K.; Kotzur, C.; Xiao, C.; Bourgeois, L.; Zhang, X.; MacFarlane, D. R., Nanostructured photoelectrochemical solar cell for nitrogen reduction using plasmon-enhanced black silicon. *Nature communications* **2016**, 7 (1), 11335.
3. Zeng, H.; Terazono, S.; Tanuma, T., A novel catalyst for ammonia synthesis at ambient temperature and pressure: Visible light responsive photocatalyst using localized surface plasmon resonance. *Catalysis Communications* **2015**, 59, 40-44.
4. Zhang, J.; Zhang, G.; Lan, H.; Liu, H.; Qu, J., Sustainable nitrogen fixation over Ru single atoms decorated Cu₂O using electrons produced from photoelectrocatalytic organics degradation. *Chemical Engineering Journal* **2022**, 428, 130373.
5. Zhang, M.; Choi, C.; Huo, R.; Gu, G. H.; Hong, S.; Yan, C.; Xu, S.; Robertson, A. W.; Qiu, J.; Jung, Y., Reduced graphene oxides with engineered defects enable efficient electrochemical reduction of dinitrogen to ammonia in wide pH range. *Nano Energy* **2020**, 68, 104323.
6. Silveira, V. R.; Bericat-Vadell, R.; Sá, J., Photoelectrocatalytic conversion of nitrates to ammonia with plasmon hot electrons. *The Journal of Physical Chemistry C* **2023**, 127 (11), 5425-5431.
7. Guo, Y.; Yang, J.; Wu, D.; Bai, H.; Yang, Z.; Wang, J.; Yang, B., Au nanoparticle-embedded, nitrogen-deficient hollow mesoporous carbon nitride spheres for nitrogen photofixation. *Journal of Materials Chemistry A* **2020**, 8 (32), 16218-16231.

8. Li, J.; Chen, R.; Wang, J.; Zhou, Y.; Yang, G.; Dong, F., Subnanometric alkaline-earth oxide clusters for sustainable nitrate to ammonia photosynthesis. *Nature Communications* **2022**, *13* (1), 1098.
9. Tan, L.; Yang, N.; Huang, X.; Peng, L.; Tong, C.; Deng, M.; Tang, X.; Li, L.; Liao, Q.; Wei, Z., Synthesis of ammonia via electrochemical nitrogen reduction on high-index faceted Au nanoparticles with a high faradaic efficiency. *Chemical Communications* **2019**, *55* (96), 14482-14485.